Photochemical & Photobiological Sciences (2026) 25:103–115
https://doi.org/10.1007/s43630-025-00829-1

RESEARCH

Beta-lactam antibiotics under light: optical and photochemical characterization

Renata Salani[1] · Alessandro Melo Deana[1] · Silvia Cristina Ñunez[2] · Celine Frochot[3] · Daniela de Fátima Teixeira Silva[4] · Christiane Pavani[1,5]

Received: 17 September 2025 / Accepted: 1 December 2025 / Published online: 15 December 2025

Abstract

Antibiotics (ATBs) remain a cornerstone in the treatment of bacterial infections, yet clinical practice increasingly incorporates photonic therapies such as photobiomodulation (PBM) and photodynamic therapy (PDT). These modalities, widely used in infectious and inflammatory conditions, are frequently administered concomitantly with ATBs. However, the potential photochemical interactions between β-lactam ATBs and light-based therapies remain poorly understood, raising questions about efficacy and safety in combined treatment settings. In this study, we characterized the optical and photochemical properties of representative β-lactam ATBs, including penicillins (amoxicillin, oxacillin), cephalosporins (cephalothin, cefazolin, ceftazidime, ceftriaxone, cefuroxime), and a carbapenem (meropenem). Using diffuse transmittance and reflectance spectroscopy, we calculated absorption and scattering coefficients via the Kubelka–Munk function. Reactive oxygen species (ROS) generation was assessed under direct blue light (460 nm) illumination and red light exposure in the presence of methylene blue (MB), a clinically employed photosensitizer. Cephalosporins demonstrated significant ROS generation under blue light, whereas penicillins and meropenem did not. In PDT-like conditions, meropenem enhanced MB-mediated ROS production and promoted MB photobleaching, suggesting potentiation of PDT effects. In contrast, penicillins suppressed MB-driven ROS generation, potentially limiting PDT efficacy. Cephalosporins showed heterogeneous effects, either enhancing, reducing, or leaving MB-induced ROS unchanged. These findings indicate that β-lactam ATBs exert distinct photobiological behaviors with potential clinical consequences. Cephalosporins may act as intrinsic photosensitizers, meropenem may potentiate PDT, and penicillins may attenuate phototherapy efficacy. Recognizing such interactions is critical to optimizing combined ATB–phototherapy regimens and avoiding unintended antagonism or toxicity in clinical practice.

Keywords Optical properties · Antibiotics · Kubelka–Munk · Transmittance · Reflectance · Photobiomodulation · Photodynamic therapy

✉ Christiane Pavani
chrispavani@gmail.com; chrispavani@uni9.pro.br

Renata Salani
salanire77@gmail.com

Alessandro Melo Deana
amdeana@uni9.pro.br

Silvia Cristina Ñunez
silvianunez@uol.com.br

Celine Frochot
celine.frochot@univ-lorraine.fr

Daniela de Fátima Teixeira Silva
fatesi@uol.com.br

[1] Postgraduate Program in Biophotonics-Medicine, Universidade Nove de Julho - UNINOVE, São Paulo, Brazil

[2] Department of Bioengeneering, Universidade Brasil, São Paulo, Brazil

[3] Université de Lorraine, CNRS, F-54000 Nancy, France

[4] Center for Lasers and Applications, IPEN – CNEN/SP, São Paulo, Brazil

[5] Universidade Nove de Julho - UNINOVE, 235/249 Vergueiro Street, Liberdade, Sao Paulo, SP 01504-001, Brazil

1 Introduction

Antibiotics (ATBs) are pharmacological agents widely used to treat bacterial infections and play a fundamental role in reducing morbidity and mortality, preventing complications, and mitigating the spread of antimicrobial resistance [1]. Among all classes, β-lactam ATBs, which include penicillins and cephalosporins, account for approximately 65% of the world's market for ATBs [2]. Despite their well-established efficacy, the potential interaction between ATBs and light-based therapeutic strategies remains an underexplored area of research.

Light-based technologies, including photobiomodulation (PBM) and photodynamic therapy (PDT), have been increasingly employed in various medical applications, such as infection control [3], wound healing [4], inflammation modulation [5], and pain management [6]. The therapeutic efficacy of these modalities is governed by the interaction between light and biological tissues, which is influenced by fundamental optical properties such as reflection, refraction, absorption, scattering, and transmission [7]. PDT, in particular, relies on the generation of reactive oxygen species (ROS) as potent antimicrobial agents, and its success depends on factors such as the optical characteristics of the treatment environment and potential interactions with pharmacological agents [8].

Given that patients undergoing PBM or PDT may simultaneously receive ATB therapy, investigating the optical properties of these drugs is essential. Certain ATBs may exhibit light absorption or scattering properties that could influence the penetration and effectiveness of therapeutic light. Moreover, some ATBs possess photosensitive molecular structures that can undergo photophysical or photochemical interactions when exposed to light, potentially altering their antimicrobial efficacy or interfering with light-based treatments. Despite these theoretical considerations, studies characterizing the optical properties of ATBs or evaluating their impact on photonic therapies are still limited in number and scope.

To characterize the optical behavior of a substance, key parameters such as the absorption coefficient (μa), reduced scattering coefficient (μ's), and reduced attenuation coefficient (μ't) must be determined [9]. The Kubelka–Munk (K–M) model is one of the most widely used technique for this purpose, enabling the quantification of these coefficients through diffuse transmittance (Td) and reflectance (Rd) measurements [10]. Understanding the optical properties of ATBs is crucial not only for assessing their compatibility with light-based therapies but also for identifying potential contraindications and optimizing treatment protocols.

Furthermore, PDT is widely used as an adjuvant antimicrobial strategy, often in combination with ATBs therapy. Methylene blue (MB) is one of the most frequently employed photosensitizers in PDT because of its well-documented antimicrobial activity cost-effectiveness [11]. However, there is a lack of studies that systematically investigated whether ATBs influence the photophysical properties of MB or its capacity to generate ROS. Similarly, blue light has been extensively studied for its intrinsic antimicrobial properties [12], yet the literature lacks data on how ATBs may interact with this light or whether such interactions could enhance or hinder its antimicrobial effects.

Given this context, this study aims to characterize the optical properties of various β-lactam ATBs, including those commonly used in both hospital and outpatient settings. Additionally, we aimed to evaluate the potential impact of these drugs on the antimicrobial efficacy of blue light and MB-mediated PDT. By elucidating these interactions, this research may contribute to optimizing combined therapeutic approaches and ensuring the safe and effective integration of ATBs with light-based antimicrobial strategies.

2 Methods

2.1 Chemicals

The MB powder (MM 319.85 g/mol) and p-nitrosodimethylaniline (RNO, MM 150.18 g/mol) were acquired from Sigma–Aldrich®. Both solutions were prepared in Milli-Q® water. The following ATBs were used: amoxicillin (500 mg, capsule, generic, Aurobindo laboratory, molar mass (MM) 365.40 g/mol), cephalothin sodium (1 g, powder, Keflin®, ABL Brasil, MM 396.42 g/mol), ceftazidime pentahydrate (1 g, powder, Kefadim®, ABL Brasil, MM 636.7 g/mol), sodium cefazolin (1 g, powder, Kefazol®, ABL Brasil, MM 476.49 g/mol), sodium cefuroxime (750 mg, powder, Zinacef®, Glaxosmithkline Brasil, MM 446.37 g/mol), ceftriaxone (1 g, powder, Rocefin®, Roche, MM 661.60 g/mol), meropenem (1 g, powder, Meronem®, Pfizer, MM 437.51 g/mol), sodium oxacillin (500 mg, powder, generic, Blau Farmacêutica laboratory, MM 423.42 g/mol. Injection-grade powders (oxacillin, ceftriaxone, cefazolin and cephalothin) contained no added excipients. Cefuroxime was supplied as a lyophilized powder with nitrogen fill. Meropenem and ceftazidime included sodium carbonate anhydrous as a buffering salt and amoxicillin capsules contained microcrystalline cellulose and magnesium stearate as excipients.

2.2 Preparation of ATBs solutions

ATBs acquired in tablets were first macerated for later solubilization. ATBs obtained in powder and liquid/solutions were directly solubilized in water. Finally, only the internal contents of the ATBs present in the capsules, which were composed of powder, were solubilized. All ATBs solutions were prepared in Milli-Q® water at a final concentration of 10×10^{-3} mol/L. After preparation, the ATBs solutions were protected from light and used immediately. The structural formulas of the ATBs are presented at Fig. 1.

2.3 Diffuse transmittance and reflectance measurements of ATBs

A USB2000 + spectrophotometer (Ocean Optics®, USA) was used to register the diffuse transmittance (Td) and reflectance (Rd) spectra of each ATBs. For this purpose, quartz cuvettes with an optical path of 1.0 cm were used, and the data were registered in the range of 400–1000 nm and the measurements were performed in triplicate. From the Td and Rd spectra that were recorded directly by the spectrophotometer, the values of the absorption coefficient, reduced scattering coefficient and reduced attenuation coefficient of each ATB were calculated via the Kubelka–Munk (K-M)[10] function. The optical parameters were derived from diffuse transmittance and reflectance data using the Kubelka–Munk two-flux approximation, allowing quantitative separation of absorption and scattering components [13]. Full equations and theoretical background are provided in Supplementary Information.

Also, Principal Component Analysis (PCA) was employed due to the high dimensionality and inherent correlations within the spectral dataset [14]. Unlike clustering algorithms such as K-Means, which are based on Euclidean distance and can be adversely affected by correlated variables, PCA effectively reduces dimensionality while preserving the variance structure of the data. Additionally, K-Means requires a predefined number of clusters, which may limit its use in exploratory spectral analyses without predefined assumptions. In contrast, PCA enables an unsupervised exploration of the data without prior assumptions. Importantly, the principal components derived from PCA can often be linked to underlying physical or chemical characteristics in the spectra, providing interpretable insights that clustering methods may not offer.

2.4 Reactive oxygen species production by MB-PDT combined to ATBs

A quartz cuvette was filled by ATB solution as previously described, MB solution (final concentration of 10.4 µmol/L) and RNO solution (final concentration of 4×10^{-5} mol/L). The absorbance was measured with a spectrophotometer (UV-1800 Schimadzu, Japan) followed by 12 cycles of 1 min of illumination with a red laser Quantum, Eccofibras, Brazil (660 nm, 89 mW, 307 mW/cm^2, 5.3 J per cycle of 60 s, 64 J total, 18 J/cm^2 per cycle, area 0.29 cm^2). The experiments were performed in triplicate at 25 °C, in an air atmosphere and in the absence of environment light. Changes in the RNO absorption determined via spectroscopy were used to calculate the reaction constant, which is directly proportional to the concentration of ROS generated [15].

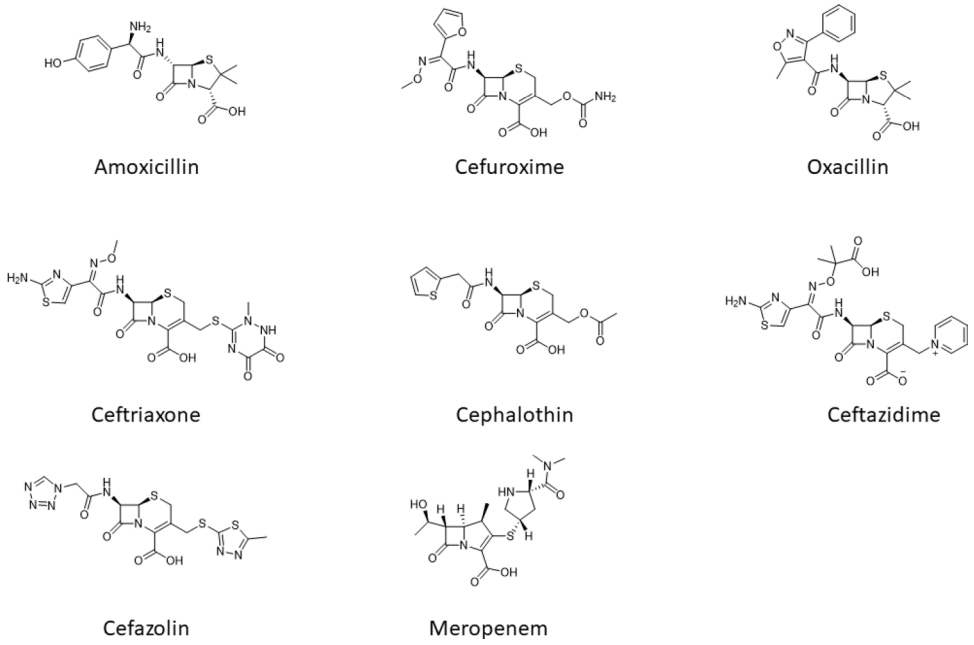

Fig. 1 Chemical structure of the ATBs studied

Table 1 Values in mean and standard deviation of the coefficients of absorption (μa), reduced scattering (μ's) and reduced Attenuation (μ't) as a function of the wavelengths (λ) 450 nm, 530 nm and 590 nm in each ATB studied

ATBs	λ 450 nm			λ 530 nm			λ 590 nm		
	μa (cm^{-1})	μ's (cm^{-1})	μ't (cm^{-1})	μa (cm^{-1})	μ's (cm^{-1})	μ't (cm^{-1})	μa (cm^{-1})	μ's (cm^{-1})	μ't (cm^{-1})
Amoxicillin	0.11 ± 0,02	0.30 ± 0.20	0.41 ± 0.21	0.11 ± 0.03	0.28 ± 0.18	0.39 ± 0.20	0.11 ± 0.03	0.27 ± 0.18	0.38 ± 0.20
Oxacillin	0.23 ± 0.02	0.30 ± 0.13	0.53 ± 0.16	0.24 ± 0.03	0.28 ± 0.11	0.52 ± 0.14	0.25 ± 0.03	0.27 ± 0.11	0.52 ± 0.14
Cephalothin	0.14 ± 0,02	0.29 ± 0.13	0.44 ± 0.14	0.14 ± 0.03	0.27 ± 0.11	0.42 ± 0.13	0.14 ± 0.03	0.26 ± 0.10	0.41 ± 0.13
Cefazolin	0.16 ± 0.03	0.30 ± 0.14	0.46 ± 0.17	0.17 ± 0.04	0.27 ± 0.12	0.44 ± 0.16	0.17 ± 0.05	0.27 ± 0.11	0.44 ± 0.15
Cefuroxime	0.17 ± 0.16	0.70 ± 0.70	0.88 ± 0.94	0.15 ± 0.14	0.61 ± 0.65	0.77 ± 0.78	0.14 ± 0.12	0.56 ± 0.57	0.71 ± 0.70
Ceftriaxone	0.12 ± 0.02	0.30 ± 0.12	0.42 ± 0.14	0.11 ± 0.03	0.28 ± 0.11	0.40 ± 0.13	0.12 ± 0.03	0.28 ± 0.10	0.40 ± 013
Ceftazidime	0.14 ± 0.02	0.30 ± 0.13	0.44 ± 0.14	0.14 ± 0.02	0.28 ± 0.11	0.42 ± 0.13	0.15 ± 0,03	0,27 ± 0,10	0,42 ± 0,13
Meropenem	0.18 ± 0.02	0.29 ± 0.13	0.47 ± 0.15	0.18 ± 0.03	0.27 ± 0.11	0.46 ± 0.14	0.18 ± 0.04	0.27 ± 0.10	0.46 ± 0.14

Table 2 Values in mean and standard deviation of the coefficients of absorption (μa), reduced scattering (μs) and reduced Attenuation (μ't) as a function of the wavelengths (λ) 660 nm, 780 nm and 810 nm in each ATB studied

ATBs	λ 660 nm			λ 780 nm			λ 810 nm		
	μa (cm^{-1})	μ's (cm^{-1})	μ't (cm^{-1})	μa (cm^{-1})	μ's (cm^{-1})	μ't (cm^{-1})	μa (cm^{-1})	μ's (cm^{-1})	μ't (cm^{-1})
Amoxicillin	0.10 ± 0.03	0.28 ± 0.17	0.38 ± 0.20	0.11 ± 0.03	0.27 ± 0.17	0.38 ± 0.20	0.11 ± 0.04	0.27 ± 0.17	0.39 ± 0.20
Oxacillin	0.24 ± 0.04	0.27 ± 0.10	0.52 ± 0.14	0.26 ± 0.04	0.25 ± 0.09	0.52 ± 0.13	0.26 ± 0.05	0.25 ± 0.09	0.52 ± 0.14
Cephalothin	0.15 ± 0.03	0.26 ± 0.09	0.42 ± 0.13	0.16 ± 0.04	0.25 ± 0.08	0.42 ± 0.12	0.17 ± 0.04	0.25 ± 0.09	0.43 ± 0.13
Cefazolin	0.17 ± 0.05	0.26 ± 0.10	0.44 ± 0.15	0.19 ± 0.05	0.24 ± 0,09	0.44 ± 0.14	0.19 ± 0.06	0.25 ± 0.09	0.45 ± 0.15
Cefuroxime	0.14 ± 0.11	0.52 ± 0.51	0.66 ± 0.62	0.14 ± 0.09	0.45 ± 0.40	0.59 ± 0.49	0.13 ± 0.09	0.45 ± 0.40	0.59 ± 0.48
Ceftriaxone	0.12 ± 0.03	0.27 ± 0.09	0.39 ± 0.13	0.13 ± 0.04	0.25 ± 0.08	0.39 ± 0.12	0.14 ± 0.04	0.26 ± 0.08	0.40 ± 0.13
Ceftazidime	0.15 ± 0.03	0.27 ± 0.10	0.42 ± 0.13	0.16 ± 0.03	0.25 ± 0.09	0.42 ± 0.12	0.16 ± 0.04	0.26 ± 0.09	0.42 ± 0.13
Meropenem	0.18 ± 0.04	0.26 ± 0.10	0.45 ± 0.14	0.20 ± 0.04	0.24 ± 0.09	0.45 ± 0.13	0.20 ± 0.05	0.25 ± 0.09	0.46 ± 0.14

2.5 Reactive oxygen species production by ATBs activated by blue light

A quartz cuvette with a 1 cm optic path was filled with 3 mL of the ATB solution previously prepared (10×10^{-3} mol/L) and the RNO solution (final concentration of 4×10^{-5}mol/L) [16, 17]. The absorbance was measured with a spectrophotometer (UV-1800 Schimadzu, Japan) followed by 12 cycles of 1 min illumination with blue LED Quantum, Eccofibras, Brazil (460 nm, 130 mW, 245 mW/cm^2, 7.8 J per cycle of 60 s, 94 J total, 14.1 J/cm^2 per cycle, area 0.53 cm^2). The experiments were performed in triplicate at 25 °C, in an air atmosphere and in the absence of environmental light.

2.6 Statistical analysis

Principal component analysis (PCA) was performed in Python via the Orange Data Mining interface, version 3.38.1. The PCA was configured with two principal components, as these proved sufficient to explain at least 95% of the variance among the samples. Additionally, the y-axis was not normalized so that the coefficients calculated via the K–M method would remain unchanged. Kinetic constants were compared via one-way ANOVA followed by Tukey's post hoc test (SPSS 30, IBM statistics), and a significance level of $\alpha < 0.05$ was used.

3 Results

3.1 Optical properties of ATBs

The values of μa, μ's and μ't of the ATBs (Tables 1 and 2) are presented at λ 450, 530, 590, 660, 780 and 810 nm. The choice of the wavelengths for evaluation was based upon the wavelengths most commonly used in photonic therapies (PBM and antimicrobial PDT). The transmittance spectrum of Milli-Q water in a quartz cuvette confirmed negligible absorption within the analyzed range (200–1000 nm), ensuring that the observed spectral features were attributable solely to the ATB samples (Supplementary Figure S1).

It can be inferred that ATBs, at the wavelengths studied, scatter more photons than they absorb. This is because the analyzed ATBs presented high attenuation coefficient values, and if the absorption coefficient presented modest values, the main contribution to attenuation must come from scattering. In fact, the scattering coefficient was approximately twice as large as the absorption coefficient at all wavelengths and for all ATBs, except for oxacillin, whose values were similar between these two coefficients. One consequence of these findings is the transmittance values: the higher the attenuation is, the lower the transmittance. Antibiotics whose absorption coefficients were approximately half of the scattering coefficient exhibited a transmittance

above 50%. On the other hand, oxacillin presented a transmittance of at most 48%.

Additionally, analysis of the optical properties was performed by dividing the wavelengths into two regions: 280 nm to 400 nm and 400 nm to 1000 nm. The region from 280 to 400 nm corresponds to ultraviolet B (280–315 nm) and ultraviolet A (315–400 nm) radiation [18]. The range between 400 and 1000 nm corresponds to the wavelengths most often used in photonic therapies, whether with lasers or LEDs [18]. All optical coefficients were analyzed using PCA. However, the absorption coefficient spectra were specifically highlighted in Fig. 2, as this parameter is the most directly related to the potential photochemical effects of the ATBs under light exposure.

The y-axis scale, which corresponds to the absorption coefficient values, clearly shows that the ATBs absorb more in the UV region than in the therapeutic window region (Fig. 2A and B, respectively). Analyzing the absorbance of the ATBs in the UV region, two principal wavelengths explain 95% of the variance among them, the absorption coefficients measured at 310 nm and 342 nm. Amoxicillin and oxacillin presented the lowest absorption in this region, followed by cephalothin.

For the wavelengths of the therapeutic window, two principal wavelengths explained 98% of the variance in the absorbances among the ATBs, the absorption coefficients at 938 nm and 1000 nm. Oxacillin exhibited the highest absorption in the visible region, followed by meropenem and cefazolin. Cefuroxime, ceftriaxone, and amoxicillin presented the lowest absorption in this region.

Among the main wavelengths used in photonic therapies, namely, 450, 530, 590, 660, 780, and 810 nm, the optical properties at 450 nm are the most important, as they explain 99% of the variance among ATBs. Cefuroxime exhibited the highest values for the scattering and attenuation coefficients, while its transmittance was among the lowest recorded (Fig. 3).

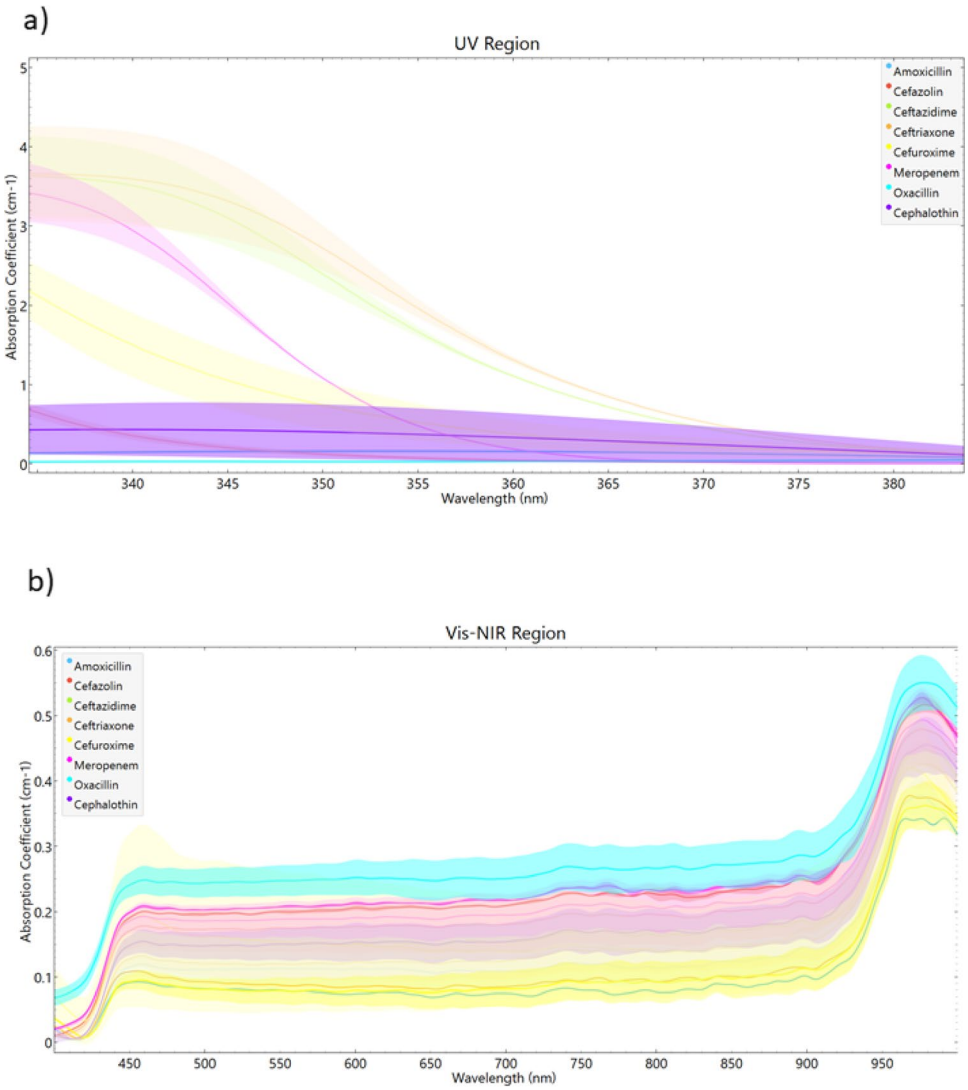

Fig. 2 Spectrum of the absorption coefficients of the studied ATBs. The shaded areas represent the standard deviation around the mean, with the mean shown as a solid line. **A** UV from 280 to 400 nm; the most prominent curves (oxacillin, amoxicillin, and cephalothin) are those differentiated by PCA. **B** at the therapeutic window, from 400 to 1000 nm. The most prominent curves (oxacillin, meropenem, cefazolin, cefuroxime, ceftriaxone, and amoxicillin) are those differentiated by the PCA

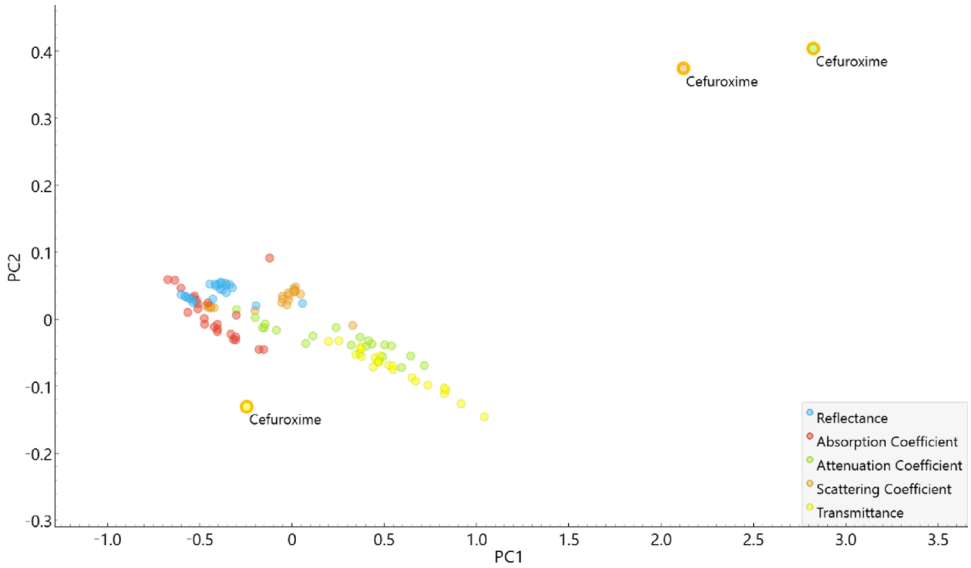

Fig. 3 Optical properties at 450 nm as a function of the principal components. Cefuroxime stands out by presenting the highest values of scattering and attenuation coefficients, while its transmittance was one of the lowest recorded

Table 3 Kinetic constant for RNO reduction when ATBs are illuminated with a blue LED (K_{LED}) or when PDT is performed with MB in the presence of (ATB K_{PDT}); MB bleaching upon irradiation (K_{MB})

ATBs	K_{LED} ($_x10^{-4}$)	K_{PDT} ($_x10^{-4}$)	K_{MB} ($_x10^{-4}$)
RNO	0.0875 ± 0.00188	–	–
MB	–	11.08 ± 1.80	2.79 ± 0.15
Amoxicillin	−0.0494 ± 0.201 n.s.	4.93 ± 0.37$^{\#}$	1.22 ± 0.52 n.s.
Oxacillin	−0.0722 ± 0.0241 n.s.	3.72 ± 0.64$^{\#}$	4.47 ± 0.38 n.s.
Cephalothin	9.158 ± 0.605*	14.10 ± 1. 60 n.s.	0.84 ± 0.08 n.s.
Cefazolin	5.818 ± 0.540*	16.73 ± 0.58*	0.95 ± 0.09 n.s.
Cefuroxime	3.245 ± 0.134*	18.27 ± 2.25*	3.41 ± 0.92 n.s.
Ceftriaxone	3.106 ± 0.147*	7.18 ± 0.11$^{\#}$	0.41 ± 0.15 n.s.
Ceftazidime	4.059 ± 0.598*	10.41 ± 1. 02 n.s.	1.72 ± 0.37 n.s.
Meropenem	0.232 ± 0.219 n.s.	31.20 ± 2.40*	11.9 ± 3.04$^{\&}$

n.s Not significant ($p>0.05$)

$^{*}p<0.05$, increased ROS production versus the control

$^{\#}p<0.05$, reduced ROS production versus the control

$^{\&}p<0.05$, increased MB bleaching versus the absence of ATB

3.2 Reactive oxygen species production

Considering that ATBs absorbs blue light, the decrease in the RNO absorption maximum upon illumination was considered a signal of ROS production. Based on the changes in RNO absorbance at 440 nm observed when the ATBs solutions were exposed to blue light (SI, Figure S2), the kinetic constant (K_{LED}) of RNO bleaching was calculated for each ATB to classify their ROS production (Table 3). The values of the kinetic constant of RNO degradation upon blue light exposure revealed that the highest to lowest levels of ROS were produced by Cephalothin (9.16 ± 0.60), Cefazolin (5.82 ± 0.54), Ceftazidime (4.06 ± 0.60) and Ceftriaxone (3.11 ± 0.15). The level of ROS produced by cefuroxime (3.25 ± 0.13) was not significantly different from that produced by ceftazidime or ceftriaxone. Amoxicillin, oxacillin and meropenem did not affect ROS production upon blue light exposure. The RNO solution exposed to blue light alone, used as the negative control (SI, Figure S3), confirmed that the photobleaching effect was dependent on the presence of photoactive ATBs.

Considering the interaction between MB and the ATBs and its impact on ROS production, the changes in RNO absorbance at 440 nm upon exposure of MB + ATB solutions to red light (SI, Figure S4) were analyzed. The kinetic constants of RNO degradation under red-light irradiation (Table 3, K_{PDT}) revealed three distinct outcomes: no change in ROS production, an increase in ROS production and a reduction in ROS production. The kinetic constant for MB was 11.08 ± 1.80, and lack of difference was observed when MB was combined with cephalothin (14.10 ± 1.60) or ceftazidime (10.41 ± 1.02). Meropenem resulted in the greatest increase in ROS production (31.20 ± 2.40), whereas cefuroxime (18.27 ± 2.25) and cefazolin (16.73 ± 0.58) increased to a similar extent. Ceftriaxone, amoxicillin and oxacillin reduced the ROS production of light-activated MB. The positive control (RNO + MB + red light; SI Figure S3) exhibited the expected bleaching profile, confirming the reliability of the assay and validating that the changes observed in MB + ATB systems reflect genuine photochemical modulation rather than experimental variability.

Photosensitizers are known to suffer photobleaching upon irradiation. Thus, the constant for MB bleaching was determined in the absence and presence of all ATBs studied (Table 3, K_{MB}). Meropenem significantly increased MB bleaching (11.9 ± 3.04), whereas the other ATBs presented no difference in K_{MB} values.

4 Discussion

The aim of this study was to investigate the optical properties of β-lactam ATBs and their impact on the antimicrobial effects of blue light and MB-mediated PDT. β-lactam ATBs share a common chemical structure, the β-lactam ring, which consists of three-carbon and one-nitrogen cyclic cores, as presented in Fig. 1 [2]. However, structural variations in the side chains can differentiate them into distinct classes. In this study, representative ATBs from different β-lactam classes, including penicillins (amoxicillin and oxacillin), cephalosporins from various generations (first generation: cephalothin and cefazolin; second generation: cefuroxime; third generation: ceftazidime and ceftriaxone), and carbapenems (meropenem), were analyzed. This classification reflects both their chemical structures and their spectra of activity as well as their pharmacokinetic characteristics.

Amoxicillin and oxacillin are penicillins. Amoxicillin has a relatively broad antimicrobial spectrum but is susceptible to degradation by beta-lactamases, whereas oxacillin has been modified to resist penicillinase (beta-lactamase) produced by some staphylococci, making it a key agent in the treatment of methicillin-sensitive *S. aureus* (MSSA) infections [19]. Usually, penicillins present limited stability in aqueous solutions [20]. Cephalothin and cefazolin belong to the first generation of cephalosporins. They exhibit strong activity against gram-positive bacteria, with more limited coverage of gram-negative bacteria [21]. Cefuroxime is a second-generation cephalosporin that has a broad spectrum of effects on both gram-positive and gram-negative bacteria [22]. Ceftazidime and ceftriaxone are examples of third-generation cephalosporins. Both have a broader spectrum for gram-negative bacteria; however, ceftazidime stands out for its activity against *Pseudomonas aeruginosa*, whereas ceftriaxone has a prolonged half-life, allowing for simplified dosing regimens (for example, once-daily administration), which makes it widely used in systemic infections. Meropenem belongs to the carbapenem class, which generally has the broadest spectrum among beta-lactams [23]. It is highly resistant to most beta-lactamases and affects a wide range of pathogens, including many that are resistant to other agents in this family. This robustness makes meropenem a preferred option for severe and hospital-acquired infections, which often involve multiresistant bacteria.

Optical properties, such as absorption and transmission, play a key role in understanding how radiation interacts with different media or tissues, and this is no different for ATBs. The number of photons penetrating the medium varies depending on the wavelength and type of ATB. After the initial reflection in the air-medium interface, the remaining photons penetrate the ATB sample; however, the degree of scattering and absorption can also vary depending on the wavelength. Shorter wavelengths undergo more Mie scattering—a type of light scattering caused by particles with sizes similar to the wavelength [24]. The next challenge for the photons is absorption itself, since the greater the absorption of a particular wavelength is, the lower its transmittance.

Unfortunately, to our knowledge, the literature lacks works on the optical properties of ATBs in the visible and near-infrared ranges, which makes comparing our findings more difficult. However, in a study on the optical properties of biological tissue, the authors emphasized that transmittance depends on combined factors such as scattering, absorption, and turbulence [25]. Scattering disperses photons in different directions distributing the radiant energy on a broader volume within the target, but reducing the foreword light transmission, which decreases transmittance [26]. However, in the present study, the Td was measured rather than the collimated transmittance, which can increase due to greater scattering, as previously indicated. Thus, the results found here are consistent with the fundamentals of optical properties and indicate that the ATBs studied here are highly scattering media between 400 and 1000 nm, except for oxacillin, which absorbs and scatters in a similar manner.

Although samples were chemically soluble in water at 10 mM, diffuse transmittance and reflectance measurements revealed measurable scattering, indicating that the solutions were not optically transparent in the Beer–Lambert sense. Under these conditions, the K–M approach is appropriate because it describes light propagation in scattering media by separating absorption (μa) and scattering (μ's) contributions, allowing a more accurate characterization of the optical properties of β-lactam ATBs. This methodology has been increasingly applied to biological and pharmaceutical systems where scattering cannot be neglected.

Although the ATBs used in this study were commercially formulated, the potential influence of excipients on the optical data appears negligible. Most samples (oxacillin, ceftriaxone, cefazolin, and cephalothin) were excipient-free powders, and the buffering salts present in meropenem and ceftazidime (sodium carbonate) are highly water-soluble and exhibit UV/Vis absorption only in the ultraviolet region (185, 233, 255, and 356 nm) [27]. Considering that the concentration of sodium carbonate was markedly lower than that of the active ATB compounds, only a minor influence of this component, if any, may have occurred. Amoxicillin was the only ATB obtained from oral capsules containing microcrystalline cellulose and magnesium stearate, which can theoretically alter light scattering depending on particle size and dispersion [28, 29]. However, the scattering and absorption coefficients obtained for amoxicillin were comparable to those of the other β-lactam ATBs, indicating that any contribution from these excipients was minimal. Overall,

the optical parameters reported here primarily reflect the intrinsic properties of the β-lactam molecules themselves. The similar absorption profiles observed among different β-lactams are consistent with the presence of common chromophores—such as the β-lactam ring and conjugated amide groups—and the predominance of scattering effects in the visible and NIR regions, where molecular absorption is intrinsically low [30, 31].

When the interaction of radiation with ATBs is studied, the literature tends to focus more on the UV spectral range than on the visible range, mainly due to the higher absorption of these drugs in that region than in the visible and near-infrared ranges [32]. In fact, the ATBs studied here absorbed approximately 10 times more UV radiation than other wavelengths did. Additionally, owing to this absorption, some ATBs may cause photosensitivity and phototoxicity [33]. The molecular mechanisms leading to photosensitivity in certain ATBs involve the capacity of these compounds to absorb UV/Vis radiation due to the presence of conjugated systems and aromatic groups. This is followed by the formation of excited states—especially triplet states—which interact with oxygen to generate ROS and catalyze photochemical reactions. These reactions can culminate in photodegradation, isomerization, or interaction with cellular components, thereby compromising both the stability of the drug and the integrity of the affected cells [33]. Nonetheless, light absorption in the visible range may also be responsible for ROS generation.

Cephalothin and cefazolin may be associated with phototoxic reactions in patients [34]. This occurs because certain structural characteristics present in first-generation cephalosporins can facilitate the absorption of UV radiation, promoting the formation of ROS that lead to skin damage. Also, this ROS production may cause ATBs degradation. In these ATBs, the structure of the side groups can cause a redshift—an absorption shift toward longer wavelengths—making the molecule also reactive to visible radiation. Indeed, cefazolin presented one of the highest absorption coefficients in the visible region. Although cephalosporins, in general, tend to cause phototoxicity more frequently, the incidence of cefuroxime, a second-generation cephalosporin, tends to be lower or less frequent than that reported for first-generation cephalosporins [35]. With respect to third-generation cephalosporins, there are no reports of phototoxicity for ceftriaxone, whereas ceftazidime increases patient susceptibility to sunburn [36]. The phototoxicity of both penicillins and carbapenems has not been reported.

Therefore, the essential difference among these ATBs lies in the subclass to which they belong and, consequently, in their spectral properties. Among the listed ATBs, cephalosporins tend to have greater photosensitizing potential than, for example, penicillins (such as amoxicillin) or carbapenems (such as meropenem), which possess distinct structural and pharmacokinetic characteristics that do not significantly favor such adverse reactions [37]. Indeed, the generation of ROS upon the activation of β-lactam ATBs with blue LED light was observed primarily in cephalosporins, which are derivatives of 7-aminocephalosporanic acid. This core structure consists of a β-lactam ring fused to a dihydrothiazine ring, with molecular variations determined by the composition of their side chains. Nonetheless, oxacillin and meropenem, did not present light absorption in the visible range and, consequently, did not generate ROS when exposed to blue LEDs, whereas amoxicillin presented some absorption in the visible range and did significantly generated ROS, as can be observed in Figure S2 (SI).

Blue light–induced antimicrobial effects have been largely attributed to the excitation of endogenous bacterial chromophores, particularly porphyrins, which generate reactive oxygen species (ROS) upon photoactivation [38]. Other chromophores, such as flavins and carotenoids, have also been identified in common human skin microbiota strains [39]. Nonetheless, blue light has also been shown to potentiate the action of certain ATBs in planktonic cultures [38, 40]. This synergistic effect is often associated with enhanced ROS formation and increased drug uptake by bacterial cells. In agreement with these observations, our findings demonstrate that ceftazidime, which displayed ROS production upon blue light exposure, has been previously reported to exhibit enhanced bactericidal activity against *Staphylococcus aureus* when irradiated with blue light [38].

Additionally, UV and blue light illumination of tetracyclines has been reported to induce singlet oxygen generation (quantum yields below 0.1) [41] along with superoxide and hydroxyl radical formation [42]. Then, tetracyclines present dual antimicrobial action, by the conventional radical ATB mechanism and photodynamic effects by blue light activation [43]. However, when blue light was combined with tetracycline treatment in biofilm models—either before or after ATB exposure—no additive antimicrobial effect was observed, suggesting that tetracyclines did not act as photosensitizers. Instead, blue light likely acted as a photophysical disruptor of the biofilm structure, enhancing ATB efficacy in the dark [44]. Considering the limited penetration depth of blue light within biofilms, its antimicrobial impact is expected to be primarily superficial. Together, these findings indicate that blue light may modulate ATB activity through distinct mechanisms depending on bacterial organization, chromophore content, and the specific chemical structure of the ATB. In this sense, it is important to emphasize that the present study was restricted to physicochemical analyses. Although antimicrobial assays could theoretically complement the findings, their outcomes would depend strongly on experimental variables such as the bacterial strain, growth

phase, metabolic state, and medium composition, which limit clinical extrapolation. Therefore, testing a single microorganism under arbitrary conditions would not necessarily provide clinically meaningful insights. By focusing on the optical and photochemical behavior of β-lactam ATBs, this study establishes a mechanistic foundation for future biological and translational research under standardized conditions.

The generation of ROS under blue or UV light can induce structural degradation of β-lactam ATB, potentially decreasing their antimicrobial potency [45–48]. Some studies have reported photo-oxidative degradation of antibiotics under simulated solar, UV, or visible light, mediated by hydroxyl radicals, superoxide anions, or singlet oxygen [49–52]. The degradation rate depends on both the antibiotic's ability to absorb light and the amount and type of ROS generated. For instance, ceftriaxone has been shown to degrade by approximately 3% under solar radiation but up to 96% under UVA exposure [50]. Nonetheless, transient ROS production may also enhance antimicrobial efficacy when oxidative stress damages bacterial structures more efficiently than the drug itself, suggesting that photo-induced effects may be context-dependent rather than purely degradative.

The analysis of the interaction between visible light and ROS generation is crucial not only for understanding the challenges in the formulation, ATBS photolysis [35], methods of application [53] and storage of certain ATBs but also for identifying suitable combinations with photonic therapies that are less prone to photon-induced adverse effects. In hospital settings, ATBs are frequently administered via intravenous catheters, and their solutions may be exposed to ambient or artificial light during preparation, transport, or infusion. For photosensitive ATBs, such exposure can lead to photodegradation, reduced antimicrobial efficacy, or the formation of reactive photoproducts. Therefore, evaluating the photostability of β-lactam ATBs under clinically relevant light conditions is essential to ensure the safety and therapeutic efficiency of both systemic ATB therapy and its integration with light-based antimicrobial strategies.

Interestingly, when exposed to blue LED cephalothin exhibited a kinetic constant (9.52 ± 0.60) comparable to that obtained for MB irradiated at 660 nm (11.08 ± 1.80). This apparent similarity arises because the RNO method in the absence of histidine captures only the type I radical contribution. While MB produces both type I and type II ROS—with singlet oxygen production ($\Phi\Delta \approx 0.5$) in ethanol or aqueous media (monomeric form) —cephalothin generates mainly radicals through type I pathways. Hence, when focusing solely on radical-mediated oxidation, the effective bleaching kinetics of cephalothin and MB become similar, despite their fundamentally different photochemical mechanisms. These results confirm that the observed RNO bleaching rates are consistent with the intended experimental scope and do not require complementary assays to validate the mechanistic rationale of the present study.

The impact of MB-mediated PDT on ROS production strongly differed among ATBs. The carbapenem meropenem strongly increased ROS production, whereas the penicillins, amoxicillin and oxacillin, strongly reduced oxidative stress. Cephalosporine had no effect on the ROS production mediated by MB (cephalothin and ceftazidime), increased the production of ROS (cephazolin and cefuroxime) and reduced the production of ROS (ceftriaxone). These differences suggest that the impact on ROS production mediated by MB-PDT is dependent upon side chains other than the main structural core.

In this study, the RNO assay was performed without histidine or imidazole to evaluate the overall generation of ROS [15]. This choice was deliberate, as the RNO probe responds to a broad range of oxidants—including hydroxyl radicals (•OH), hydrogen peroxide, superoxide [54–58]. While the inclusion of histidine would render the assay more selective to singlet oxygen ($^1O_2$), its presence also biases the reaction toward a type II mechanism, limiting the detection of other ROS. Although MB displays a high $^1O_2$ quantum yield ($\Phi\Delta \approx 0.5$) under ideal, monomeric conditions (example: ethanol [59]), MB's photochemical behavior is strongly influenced by its aggregation state and the surrounding medium [60–62]. In aqueous and biologically relevant environments, MB tends to form dimers or higher aggregates, particularly in the presence of proteins, salts, or bacterial surfaces. Under these circumstances, type I photoreactions dominate, generating radicals such as •OH and $O_2^{\bullet -}$, which contribute significantly to bacterial inactivation [63–65]. Moreover, in hypoxic environments typical of bacterial biofilms, type I mechanisms are thermodynamically favored over $^1O_2$-dependent pathways [65]. Given that β-lactam ATBs have negligible absorbance in the red region and that tetracyclines exhibit singlet-oxygen quantum yields below 0.1 [41], a selective assay for $^1O_2$ would provide limited mechanistic insight. Therefore, employing RNO without histidine allowed us to monitor the general oxidative profile of the system, encompassing both radical and non-radical species. This strategy provides a more realistic representation of the photochemical dynamics expected when MB and ATBs coexist in bacterial or biofilm environments.

The chemical structure of meropenem presents a 1β-methyl substitution and exhibits antimicrobial action via oxidative stress induction, reaching higher levels than those of penicillins or cephalosporins do [66], which is attributed to a biological effect linked to its capacity to disrupt mitochondria and the electron transport chain. Nonetheless, in the present study, strong ROS production was induced when MB-PDT was combined with MB-PDT, an extension that

also induced increased MB photobleaching. The implications of these results should be evaluated when considering the concomitant clinical application of meropenem and MB-PDT for antimicrobial action.

Meropenem may be indicated for target skin infections, pneumonia and nosocomial pneumonia, severe infections, urinary tract infections, and other conditions [67, 68]. In some cases, combining antimicrobial treatment with a local antimicrobial strategy may be important to optimize the results. Thus, MB-mediated PDT may be helpful for preventing other or generalized infections, as well as combined treatment strategies [69]. Importantly, since meropenem increased the ROS production mediated by MB-PDT, a synergistic effect may have occurred. On the other hand, excessive ROS production may accelerate MB degradation, impairing PDT. During this study, increased MB degradation was observed, as determined by the highest degradation constant between ATBs (11.9 ± 3.04). Nonetheless, in patients, the interaction between MB and meropenem is reduced once MB is applied topically while meropenem is used systemically.

Cephalosporins present different photochemical behaviors depending on the pH of the solution, since they present ionizable groups [48]. Cefazolin and cefuroxime, for example, contain heterocyclic moieties and electron-withdrawing substituents that may facilitate energy transfer or modulate the redox state of MB, promoting ROS generation [70]. Additionally, cefazolin may undergo photolysis, generating byproducts with increased ROS generation capacity [70]. Conversely, ceftriaxone features a unique thiotriazinedione side chain, which may have acted as an ROS scavenger or interfered with MB excitation dynamics, thus reducing the ROS output. Ceftriaxone may suffer photooxidation and lose its bactericidal capacity when sensitized by riboflavin [71].

The absence of ROS modulation by cephalothin and ceftazidime indicates a lack of significant photochemical interaction with MB, suggesting a neutral photodynamic profile. These findings are particularly relevant in clinical contexts where cephalosporins are coadministered with MB-PDT, as they may potentiate, inhibit, or remain inert in relation to photodynamic ROS production. Understanding these specific interactions is crucial when designing combined antimicrobial strategies, especially in cases of resistant or recurrent infections where synergy between systemic and local therapies is desired. Further studies are warranted to elucidate the precise molecular mechanisms behind these effects and to determine their translational relevance.

In summary, penicillins and meropenem exhibited negligible direct ROS generation under blue-light illumination, whereas cephalosporins did. The RNO protocol intentionally omitted histidine, favoring the detection of radical-driven bleaching rather than $^1O_2$-mediated oxidation; therefore, the pronounced RNO loss observed for several cephalosporins under blue light is most consistently explained by type I photochemical pathways. ROS generation may have dual implications—either promoting limited photo-oxidation of the drug molecule or transiently enhancing antibacterial efficacy. Future work will address antibiotic stability and biological activity following controlled irradiation to quantify these effects.

In MB-mediated PDT, penicillins reduced ROS formation, likely acting as radical scavengers and/or triplet-state quenchers of MB, whereas meropenem not only enhanced ROS generation but also accelerated MB photobleaching. The heterogeneous responses among cephalosporins (enhancement, neutrality, or inhibition) toward MB-PDT-induced ROS production are consistent with side-chain–dependent redox and photophysical variations rather than a single, uniform mechanism. Altogether, these findings underscore the translational relevance of investigating ATB–light interactions, as such knowledge may inform clinical decision-making and guide the development of optimized protocols for combined antibiotic and photonic therapies.

5 Conclusion

This study demonstrated that β-lactam ATBs exhibit distinct optical properties and differential interactions with photonic modalities, particularly under blue and red light exposure associated with MB. The high scattering behavior observed across most ATBs within the 400–1000 nm range, with oxacillin as a notable exception, suggests that their optical behavior may influence light–tissue interactions in therapeutic contexts. Furthermore, cephalosporins—but not penicillins or carbapenems—were capable of generating ROS upon blue light exposure, indicating potential intrinsic photosensitivity under concomitant antimicrobial treatment. When combined with MB-mediated PDT, the ATBs exhibited variable effects: cephalosporins both increased, reduced and showed no effect on ROS generation; meropenem significantly enhanced both ROS generation and MB photobleaching, suggesting synergistic potential; conversely, penicillins diminished the efficacy of MB-PDT. These findings underscore the importance of evaluating the optical and photochemical behavior of ATBs prior to their concurrent use with light-based therapies, as such interactions may influence treatment outcomes, either by enhancing therapeutic efficacy or introducing antagonistic effects. Further studies are warranted to explore the clinical implications of these interactions and to inform safe and effective multimodal therapeutic strategies.

Supplementary Information The online version contains supplementary material available at https://doi.org/10.1007/s43630-025-00829-1.

Author contributions RS contributed to the conception, design of the study, acquisition of data and drafting the article. AMD, SCN and CF contributed to the analysis, interpretation of data and revising the article critically. CF prepared Fig. 1. DFTS contributed to the conception and design of the study, analysis and interpretation of data and drafting the article. DFTS prepared Figs. 2 and 3. CP contributed to the analysis, interpretation of data and drafting the article. All authors reviewed the manuscript and have approved the final version of the article.

Funding This work was supported by the Coordination for the Improvement of Higher Education Personnel (CAPES) [grant number 88887.493294/2020-00]; the National Council for Scientific and Technological Development - CNPq [grant number 305373/2023-4]; and São Paulo Research Foundation (FAPESP) [grant numbers 2015/05259-8 and 2016/03037–0].

Data availability Any raw data files needed will be available from the corresponding author upon reasonable request.

Declarations

Conflict of interest The authors declare no competing interests.

References

1. Moser, C., Lerche, C. J., Thomsen, K., Hartvig, T., Schierbeck, J., Jensen, P. Ø., Ciofu, O., & Høiby, N. (2019). Antibiotic therapy as personalized medicine – General considerations and complicating factors. *APMIS, 127*, 361–371.
2. Pandey, N., & Cascella, M. (2025). *StatPearls*. StatPearls Publishing.
3. Da Collina, G. A., Freire, F., Santos, T. P. D. C., Sobrinho, N. G., Aquino, S., Prates, R. A., Da Silva, D. D. F. T., Tempestini Horliana, A. C. R., & Pavani, C. (2018). Controlling methylene blue aggregation: A more efficient alternative to treat *Candida albicans* infections using photodynamic therapy. *Photochemical & Photobiological Sciences, 17*, 1355–1364.
4. Oliveira De Lima, T., Freitas, K. A. B. D. S., Batista Da Silva, K. A., Rodrigues, M. F. S. D., Dos Santos, T. B., Shimozato, I. A. D., Pavani, C., & Cecatto, R. B. (2024). Light-based therapies and radiodermatitis: A case series report. *EXCLI Journal, 23*, 1276–1286.
5. Escarrat, V., Reato, D., Blivet, G., Touchon, J., Rougon, G., Bos, R., & Debarbieux, F. (2024). Dorsoventral photobiomodulation therapy safely reduces inflammation and sensorimotor deficits in a mouse model of multiple sclerosis. *Journal of Neuroinflammation, 21*, 321.
6. Da Silva Oliveira, V. R., De Paula Oliveira, I., Alonso-Matielo, H., Oliveira, V. T., Kremer, J. L., Casalverini, M. C. D., Ribeiro, F. Q., Maria-Engler, S. S., Assis, S. R., Teixeira, M. J., Lotfi, C. F. P., Otoch, J. P., & Dale, C. S. (2025). Photobiomodulation therapy in diabetes: Benefits for pain relief, quality of life, and wound healing. *Photochemistry and Photobiology*. https://doi.org/10.1111/php.14053
7. Carneiro, I., Carvalho, S., Henrique, R., Oliveira, L., & Tuchin, V. V. (2019). Measuring optical properties of human liver between 400 and 1000 Nm. *Quantum Electronics*, *49*, 13–19.
8. Singh, N., & Lilge, L. (2025). Light-based therapy of infected wounds: A review of dose considerations for photodynamic microbial inactivation and photobiomodulation. *Journal of Biomedial Optics*, *30*, 030901.
9. Golovynskyi, S., Golovynska, I., Stepanova, L. I., Datsenko, O. I., Liu, L., Qu, J., & Ohulchanskyy, T. Y. (2018). Optical windows for head tissues in near-infrared and short-wave infrared regions: Approaching transcranial light applications. *Journal of Biophotonics, 11*, Article e201800141.
10. Yang, L., & Kruse, B. (2004). Revised Kubelka–Munk theory I Theory and application. *Journal of the Optical Society of America. A, Optics, Image Science, and Vision, 21*, Article 1933.
11. Bezerra, D. T., La Selva, A., Cecatto, R. B., Deana, A. M., Prates, R. A., Bussadori, S. K., Mesquita-Ferrari, R. A., Motta, L. J., Fernandes, K. P. S., Martimbianco, A. L. C., Frochot, C., Pereira, B. J., Rossi, F., Mimica, M. J., & Horliana, A. C. R. T. (2023). Antimicrobial photodynamic therapy in the nasal decolonization of maintenance hemodialysis patients: A pilot randomized trial. *American Journal of Kidney Diseases, 81*, 528-536.e1.
12. Shalaby, R. M., El-Kosery, S. M., Soliman, M. M., & Osman, D. A. (2024). Effect of blue light emitting diode therapy on recurrent vulvovaginal candidiasis: A randomized assessor-blinded controlled trial. *Physiotherapy Research International, 29*, Article e2129.
13. Sabino, C. P., Deana, A. M., Yoshimura, T. M., Da Silva, D. F. T., França, C. M., Hamblin, M. R., & Ribeiro, M. S. (2016). The optical properties of mouse skin in the visible and near infrared spectral regions. *Journal of Photochemistry and Photobiology, B: Biology, 160*, 72–78.
14. Greenacre, M., Groenen, P. J. F., Hastie, T., D'Enza, A. I., Markos, A., & Tuzhilina, E. (2022). Principal component analysis. *Nature Reviews Methods Primers, 2*, Article 100.
15. Linger, C., Lancel, M., & Port, M. (2023). Evaluation of relative efficiency of PDT photosensitizers in producing hydroxyl radicals and singlet oxygen in aqueous media using a UV–visible spectroscopy pNDA dosage. *Journal of Photochemistry and Photobiology, B: Biology, 241*, Article 112664.
16. Babu, B., Ochappan, T., Asraf Ali, T., Mack, J., Nyokong, T., & Gopalakrishnan Sethuraman, M. (2021). Photodynamic activity and photoantimicrobial chemotherapy studies of ferrocene-substituted 2-thiobarbituric acid. *Bioorganic & Medicinal Chemistry Letters, 40*, Article 127922.
17. Kraljić, I., & Trumbore, C. N. (1965). p-Nitrosodimethylaniline as an OH radical scavenger in radiation chemistry1. *Journal of the American Chemical Society, 87*, 2547–2550.
18. Serrage, H., Heiskanen, V., Palin, W. M., Cooper, P. R., Milward, M. R., Hadis, M., & Hamblin, M. R. (2019). Under the spotlight: Mechanisms of photobiomodulation concentrating on blue and green light. *Photochemical & Photobiological Sciences*, *18*, 1877–1909.
19. Kasse, G. E., Cosh, S. M., Humphries, J., & Islam, M. S. (2024). Antimicrobial prescription pattern and appropriateness for respiratory tract infection in outpatients: A systematic review and meta-analysis. *Systematic Reviews, 13*, 229.
20. Jenkins, A., Jamieson, C., & Santillo, M. (2024). Systematic review of room temperature stability of key beta-lactam antibiotics for extended infusions in inpatient settings. *European Journal of Hospital Pharmacy, 31*, 2–9.
21. Lee, B. J., Wang, S. K., Constantino-Corpuz, J. K., Apolinario, K., Nadler, B., McDanel, J. S., Scheetz, M. H., & Rhodes, N. J. (2019). Cefazolin vs. anti-staphylococcal penicillins for treatment of methicillin-susceptible *Staphylococcus aureus* bloodstream infections in acutely ill adult patients: Results of a systematic review and meta-analysis. *International Journal of Antimicrobial Agents, 53*, 225–233.

22. Omole, A. E., Awosika, A. O., & Patel, P. (2025). *StatPearls*. StatPearls Publishing.
23. Cho, J. C., Zmarlicka, M. T., Shaeer, K. M., & Pardo, J. (2018). Meropenem/Vaborbactam, the first carbapenem/β-lactamase inhibitor combination. *Annals of Pharmacotherapy, 52*, 769–779.
24. Balderas-Cabrera, C., & Castillo, R. (2024). Mie scattering theory applied to light scattering of large nonhomogeneous colloidal spheres. *Journal of Chemical Physics, 161*, 084903.
25. Jacques, S. L. (2013). Optical properties of biological tissues: A review. *Physics in Medicine and Biology, 58*, R37–R61.
26. Özcan, M. K., Gökçe, M. C., & Baykal, Y. (2025). Transmittance of Gaussian beams in biological tissues. *Journal of Quantitative Spectroscopy & Radiative Transfer*, *333*, 109312.
27. Al Omari, M. M. H., Rashid, I. S., Qinna, N. A., Jaber, A. M., & Badwan, A. A. (2016). *Profiles of drug substances, excipients and related methodology* (Vol. 41, pp. 31–132). Elsevier.
28. Yang, H., Jacucci, G., Schertel, L., & Vignolini, S. (2022). Cellulose-based scattering enhancers for light management applications. *ACS Nano, 16*, 7373–7379.
29. Yohana Chaerunisaa, A., Sriwidodo, S., & Abdassah, M. (2020). In U. Ahmad & J. Akhtar (Eds.), *Pharmaceutical formulation design - recent practices.* IntechOpen.
30. Cielecka-Piontek, J., Zalewski, P., Krause, A., & Milewski, M. (2012). In J. Uddin (Ed.), *Macro to nano spectroscopy.* InTech.
31. Vilvanathan, S. (2021). In A. Paul, N. Anandabaskar, J. Mathaiyan, & G. M. Raj (Eds.), *Introduction to basics of pharmacology and toxicology* (pp. 821–834). Springer Nature Singapore.
32. Di Bartolomeo, L., Irrera, N., Campo, G. M., Borgia, F., Motolese, A., Vaccaro, F., Squadrito, F., Altavilla, D., Condorelli, A. G., Motolese, A., & Vaccaro, M. (2022). Drug-induced photosensitivity: Clinical types of phototoxicity and photoallergy and pathogenetic mechanisms. *Frontiers in Allergy, 3*, 876695.
33. Kowalska, J., Rok, J., Rzepka, Z., & Wrześniok, D. (2021). Drug-induced photosensitivity—From light and chemistry to biological reactions and clinical symptoms. *Pharmaceuticals (Basel), 14*, 723.
34. Pandey, R., Mehrotra, S., Ray, R. S., Joshi, P. C., & Hans, R. K. (2002). Evaluation of UV-radiation induced singlet oxygen generation potential of selected drugs. *Drug and Chemical Toxicology, 25*, 215–225.
35. Osman, A. H., El-Maali, N. A., Aly, A. A. M., & Al-Hazmi, G. A. (2002). Spectral, thermal, and photochemical studies on certais first, second, and third generation cephalosporin antibiotics and their Cd (II) complexes. *Synthesis and Reactivity in Inorganic, Metal-Organic, and Nano-Metal Chemistry, 32*, 763–781.
36. Vinks, S. A. T. M. M., Heijerman, H. G. M., De Jonge, P., & Bakker, W. (1993). Photosensitivity due to ambulatory intravenous ceftazidime in cystic fibrosis patient. *Lancet, 341*, 1221–1222.
37. Gould, J. W., Mercurio, M. G., & Elmets, C. A. (1995). Cutaneous photosensitivity diseases induced by exogenous agents. *Journal of the American Academy of Dermatology*, *33*, 551–573.
38. Leanse, L. G., Anjos, C. D., Kaler, K. R., Hui, J., Boyd, J. M., Hooper, D. C., Anderson, R. R., & Dai, T. (2023). Blue light potentiates antibiotics in bacteria via parallel pathways of hydroxyl radical production and enhanced antibiotic uptake. *Advanced Science, 10*, Article 2303731.
39. Serrage, H. J., O' Neill, C. A., & Uzunbajakava, N. E. (2024). Illuminating microflora: Shedding light on the potential of blue light to modulate the cutaneous microbiome. *Frontiers in Cellular and infection Microbiology, 14*, 1307374.
40. He, Y., Huang, Y. Y., Xi, L., Gelfand, J. A., & Hamblin, M. R. (2018). Tetracyclines function as dual-action light-activated antibiotics. *PLoS One, 13*, e0196485.
41. Hasan, T., & Khan, A. U. (1986). Phototoxicity of the tetracyclines: Photosensitized emission of singlet delta dioxygen. *Proceedings of National Academy of Sciences*, *83*, 4604–4606.
42. Martin, J. P., Colina, K., & Logsdon, N. (1987). Role of oxygen radicals in the phototoxicity of tetracyclines toward *Escherichia coli* B. *Journal of Bacteriology, 169*, 2516–2522.
43. Hamblin, M. R., & Abrahamse, H. (2019). Tetracyclines: Light-activated antibiotics? *Future Medicinal Chemistry, 11*, 2427–2445.
44. Negri, L. B., Korupolu, S., Farinelli, W., Jolly, A. K., Redmond, R. W., Aggarwal, S., Rahme, L. G., Gilchrist, K. H., Anderson, R. R., & Gelfand, J. A. (2025). Antimicrobial blue light reduces Human-Wound pathogens' resistance to Tetracycline-Class antibiotics in biofilms. *Cells*, *14*, 219.
45. Qian, Y., Liu, X., Li, K., Gao, P., Chen, J., Liu, Z., Zhou, X., Zhang, Y., Chen, H., Li, X., & Xue, G. (2020). Enhanced degradation of cephalosporin antibiotics by matrix components during thermally activated persulfate oxidation process. *Chemical Engineering Journal*, *384*, 123332.
46. Reynoso, E., Nesci, A., Allegretti, P., Criado, S., & Biasutti, M. A. (2012). Kinetic and mechanistic aspects of sensitized photodegradation of β-lactam antibiotics: Microbiological implications. *Redox Report*, *17*, 275–283.
47. Timm, A., Borowska, E., Majewsky, M., Merel, S., Zwiener, C., Bräse, S., & Horn, H. (2019). Photolysis of four β–lactam antibiotics under simulated environmental conditions: Degradation, transformation products and antibacterial activity. *Science of the Total Environment*, *651*, 1605–1612.
48. Ge, L., Guo, Y., Xie, Q., Yang, Y., Zhang, P., Wang, J., & Zhu, Y. (2025). Aquatic photochemistry for different dissociation forms of cephalosporin antibiotics: Degradation kinetics, products and photo-modified toxicity. *Environmental Pollution*, *371*, 125926.
49. Bi, H., Zhou, Z., Liu, Q., Zhao, R., Chen, F., Zhang, J., & Shen, Z. (2025). Machine learning decoding of electronic thresholds in prediction of oriented generation of solar-induced oxidative reactive species and antibiotics degradation. *Journal of Hazardous Materials*, *499*, 140062.
50. Abramović, B. F., Uzelac, M. M., Armaković, S. J., Gašić, U., Četojević-Simin, D. D., & Armaković, S. (2021). Experimental and computational study of hydrolysis and photolysis of antibiotic ceftriaxone: Degradation kinetics, pathways, and toxicity. *Science of the Total Environment*, *768*, 144991.
51. Ji, J., Li, H., & Liu, S. (2025). Current natural degradation and artificial intervention removal techniques for antibiotics in the aquatic environment: A review. *Applied Sciences, 15*, Article 5182.
52. Bhuin, A., Udayakumar, S., Gopalarethinam, J., Mukherjee, D., Girigoswami, K., Ponraj, C., & Sarkar, S. (2024). Photocatalytic degradation of antibiotics and antimicrobial and anticancer activities of two-dimensional ZnO nanosheets. *Scientific Reports*, *14*, 10406.
53. Alawyia, B., Fathima, S., Spernovasilis, N., & Alon-Ellenbogen, D. (2024). Continuous versus intermittent infusion of beta-lactam antibiotics: Where do we stand today? A narrative review. *Germs*, *14*, 162–178.
54. Kraljić, I., & Trumbore, C. N. (1965). p-Nitrosodimethylaniline as an OH radical scavenger in radiation chemistry. *Journal of the American Chemical Society*, *87*, 2547–2550.
55. Kraljić, I. (1970). Photolytic determination of SO4- rate constants. *International Journal for Radiation Physics and Chemistry*, *2*, 59–68.
56. Kraljić, I. (1986). Detection of singlet oxygen and its role in dye-sensitized photooxidation in aqueous and micellar solutions. *Biochimie*, *68*, 807–811.
57. Hatada, M., Kraljic, I., El Samahy, A., & Trumbore, C. N. (1974). Radiolysis and photolysis of the hydrogen peroxide-p-nitrosodimethylaniline-oxygen system. *Journal of Physical Chemistry*, *78*, 888–891.

58. Herman, J., & Neal, S. L. (2019). Efficiency comparison of the imidazole plus RNO method for singlet oxygen detection in biorelevant solvents. *Analytical and Bioanalytical Chemistry*, *411*, 5287–5296.
59. Wilkinson, F., Helman, W. P., & Ross, A. B. (1993). Quantum yields for the photosensitized formation of the lowest electronically excited singlet state of molecular oxygen in solution. *Journal of Physical and Chemical Reference Data*, *22*, 113–262.
60. Nuñez, S. C., Yoshimura, T. M., Ribeiro, M. S., Junqueira, H. C., Maciel, C., Coutinho-Neto, M. D., & Baptista, M. S. (2015). Urea enhances the photodynamic efficiency of methylene blue. *Journal of Photochemistry and Photobiology, B: Biology, 150*, 31–37.
61. Monteiro, C. M., Gonçalves, J. M. L. A., Machado, G. B., Chiarelli-Neto, O., Prates, R. A., Frochot, C., & Pavani, C. (2025). Viscous methylene blue formulation for antimicrobial photodynamic therapy in dentistry. *Scientific Reports*, *15*, 15751.
62. Collina, G. A., Freire, F., Da Silva Barbosa, V., Bento Correa, C., Reis Nascimento, H., Ratto Tempestini Horliana, A. C., Da Silva, D. D. F. T., Araujo Prates, R., & Pavani, C. (2020). Photodynamic antimicrobial chemotherapy action of phenothiazinium dyes in planktonic *Candida albicans* is increased in sodium dodecyl sulfate. *Photodiagnosis and Photodynamic Therapy, 29*, Article 101612.
63. Junqueira, H. C., Severino, D., Dias, L. G., Gugliotti, M. S., & Baptista, M. S. (2002). Modulation of methylene blue photochemical properties based on adsorption at aqueous micelle interfaces. *Physical Chemistry Chemical Physics: Pccp*, *4*, 2320–2328.
64. Usacheva, M. N., Teichert, M. C., & Biel, M. A. (2003). The role of the methylene blue and toluidine blue monomers and dimers in the photoinactivation of bacteria. *Journal of Photochemistry and Photobiology. B, Biology, 71*, 87–98.
65. Jiang, J., Lv, X., Cheng, H., Yang, D., Xu, W., Hu, Y., Song, Y., & Zeng, G. (2024). Type I photodynamic antimicrobial therapy: Principles, progress, and future perspectives. *Acta Biomaterialia*, *177*, 1–19.
66. Ye, D., Sun, J., Jiang, R., Chang, J., Liu, Y., Wu, X., Li, L., Luo, Y., Wang, J., Guo, K., & Yang, Z. (2024). β-lactam antibiotics induce metabolic perturbations linked to ROS generation leads to bacterial impairment. *Frontiers in Microbiology, 15*, Article 1514825.
67. Moradi, H., Sajadi-Javan, Z. S., Mousavi, S., Rostami, S., & Khaniabadi, B. M. (2024). Systematic review and meta-analysis of colistin plus meropenem therapy for the treatment of nosocomial pneumonia. *Iranian Journal of Microbiology, 16*, 722–731.
68. Sivanandy, P., Manirajan, P., Wen Qi, O., Teng Khai, O., Chun Wei, O., Wei Ying, N., Wadingasafi, N. A. N., Azhar, N. A., & Nor Rohaizan, N. A. (2024). A systematic review of efficacy and safety of newer drugs approved from 2016 to 2023 for the treatment of complicated urinary tract infections. *Annals of Medicine, 56*, Article 2403724.
69. Zhao, T., Wu, X., Zhang, Q., Li, C., Worthington, H. V., & Hua, F. (2020). Oral hygiene care for critically ill patients to prevent ventilator-associated pneumonia. *Cochrane Database of Systematic Reviews, 12*, Article CD008367.
70. Wang, X. H., & Lin, A. Y. C. (2012). Phototransformation of cephalosporin antibiotics in an aqueous environment results in higher toxicity. *Environmental Science & Technology, 46*, 12417–12426.
71. Jiang, M., Wang, L., & Ji, R. (2010). Biotic and abiotic degradation of four cephalosporin antibiotics in a lake surface water and sediment. *Chemosphere*, *80*, 1399–1405.